Hybrid Gene Networks: a new Framework and a Software Environment

Emilien Cornillon[1], Jean-Paul Comet[1], Gilles Bernot[1], Gilles Enée[1]

January 26, 2016

[1] University Nice Sophia Antipolis, I3S laboratory - UMR CNRS 7271, 2000 route des lucioles, CS 40121, F-06903 Sophia Antipolis CEDEX, France

Abstract

The modelling framework of René Thomas allows one to design abstract models of gene regulatory networks. In this formalism, time is also abstracted and dynamics are represented by the *succession* of discrete events. However, for numerous gene networks, the delay between two events is of first interest (circadian clock, cell growth, *etc*). In this chapter, we present a hybrid Thomas' formalism allowing us to take into account chronometrical information. We give the definition of the formalism and we present a first version of a user-friendly software platform named HyMBioNet. The main difficulty of an hybrid framework resides in the identification of the numerous parameters it involves. We illustrate our approach with an extremely simplified network of the mammalian circadian clock. For this example, we show how to determine accurate parameters. Finally, we show some simulations obtained *via* HyMBioNet.

1 Introduction

Modelling a gene network consists in designing a virtual representation that provides a basis for the prediction of behaviours of interest. In a majority of cases, the key problem is the identification step which aims at determining the parameter values allowing a good representation of the known biological behaviours. A lot of network parameters are hard to identify and the larger the network, the more difficult the experimental determination of parameters. To overcome this difficulty, we gather information about the global behaviour of the biological complex systems, and we deduce some constraints on the parameters. Among information that can be experimentally measured, the elapsed time between two observed states is easy to evaluate and is often underused to model biological systems. In this article we propose a new hybrid formalism which gives the possibility to reflect the durations of regulations. Thus, measured elapsed times become a way to constrain the set of admissible models.

The differential equation frameworks [2, 13] rely on the hypothesis of continuity and homogeneousness of concentrations and provide very precise time information. However, the domain of parameters is infinite. Thus, an automatic formal identification of parameters is very difficult especially when the differential system is not

linear. On an other hand, the purely discrete formalisms [22, 14] make the reverse hypothesis: The concentration space is sliced into a small number of intervals, which reduces considerably the number of states and also reduces the number of values that the parameters can take. Thus the research space for parameters becomes finite and computer aided approaches based on formal logic help the modeller to find parameter values. For example, the Thomas' modelling framework [21] admits a completely automated identification step: The known behaviours are expressed in temporal logic formulas, all parameterisations are then checked by model-checking algorithm in order to select only the ones that are compatible with biological knowledge [6, 7]. Between these two classes of formalisms, some others exist [15, 1, 10] and finding a modelling frameworks that allow an automated reasoning and simplify the parameter identification step is an active research field.

The formalism presented in this chapter is an extension of the Thomas' formalism [21, 22]. Intuitively, whereas models of original Thomas' framework allow only discrete changes, the hybrid formalism presented here, in addition, mimics continuous evolutions of concentration inside each discrete state. Here, parameters can be thought as an evolution speed inside the discrete states, and the time to walk across the discrete state (at the considered speed) represents the delay mandatory inside the system to go through the discrete state.

We illustrate this formalism with the example of the mammalian circadian clock. It regulates a lot of important physiology mechanism [8]. Consequently, chronometrical time plays an important role in circadian cycle models. The circadian clock is well studied in mammals and it is often modelled with differential equations [17, 12, 3]. Each cell contains a clock which oscillates with its own period (approximately 24 hours) without stimuli. To oscillate in exactly 24 hours and synchronize with the others, cells receive *zeitgeber* inputs (synchronizers as light, temperature and food intake). The light is a very important zeitgeber and we will focus on it for the rest of this article.

The mammalian circadian clock is based on a gene regulatory network present in all cells. Here, we focus on the core of the molecular clock, composed of 4 elements: *Per* genes (*Per1, Per2, Per3*), *Cry* genes (*Cry1, Cry2*), *Bmal1* gene and *Clock* gene (or its homologue *Npas2*). Proteins of *Bmal1* and *Clock* form a complex CLOCK-BMAL1 which activates the transcription of *Per* and *Cry* genes. PER and CRY proteins are synthesized in the cytoplasm where they form complexes PER-CRY and accumulate. Once these complexes are phosphorylated, they move to the nucleus [24], where they are bound to CLOCK-BMAL1 and inhibit the activation of *Per* and *Cry* genes. The presence of light induces an activation on *Per1* and *Per2* genes [19] by acetylation of the chromatin [5, 11] and an accumulation of PER-CRY complexes in the cytoplasm.

The chapter is organised as follows. In Section 2, we define our hybrid framework and the simplify circadian clock model on which we apply it. Section 3 presents a software platform to simulate our hybrid networks. Section 4 illustrates how one can build, in our running example, the constraints on the parameters. Section 5 shows some simulation results obtained with parameters satisfying the previous constraints. Finally, we discuss the adequacy of the approach.

2 A new hybrid formalism for gene networks

Our hybrid formalism is based on the René Thomas theory, enriched with multiplexes [16]. Section 2.1 gives the formal definitions and we explain the link between our parameters and the ones of Thomas. Section 2.2 presents the hybrid states and the notion of resources. Finally, Section 2.3 defines the hybrid state space of a network.

2.1 Hybrid gene networks

As shown in Figure 1, a gene network is visualized as a labelled directed graph (interaction graph) in which vertices are either variables (within circles) or multiplexes (within rectangles). Variables abstract genes and their products, and multiplexes contain propositional formulas that encode situations in which a group of variables (inputs of multiplexes, dashed arrows) influences the evolution of some variables (output of multiplexes, plain arrows). A multiplex can encode the formation of molecular complexes, phosphorylation by a protein, competition of entities for activation of a promoter, *etc*.

To illustrate our formalism, we use a very simple abstraction of the mammalian circadian clock firstly defined in [9]. According to this abstraction, the main role of *Per* and *Cry* is to produce PER-CRY complexes and the effect of these complexes is to inhibit the *Per* and *Cry* genes. Thus, the model contains 2 variables, g represents the genes *Per* and *Cry*, and pc represent the complexes PER-CRY in the nucleus. The variable g has a positive action on pc (since the presence of pc is a consequence of the activation of the clock genes) whereas pc inhibits the variable g. During the day, light induces an accumulation of PER-CRY in the cytoplasm, preventing PER-CRY to enter the nucleus. This inhibits the inhibitory effect of pc on g.

Figure 1 shows this model: the formula associated with the multiplex m_{pc} is $(g \geqslant 1)$ which means that, when the expression level of g reaches a certain value 1, it can help the activation of the variable pc. The other multiplex, m_g is associated with the formula $\neg(pc \geqslant 1)$ which means on the contrary that pc is an inhibitor of g when it reaches the value 1. The variable L (as Light) is a zeitgeber, an external variable that will be controlled during simulations. Consequently, it has no predecessor.

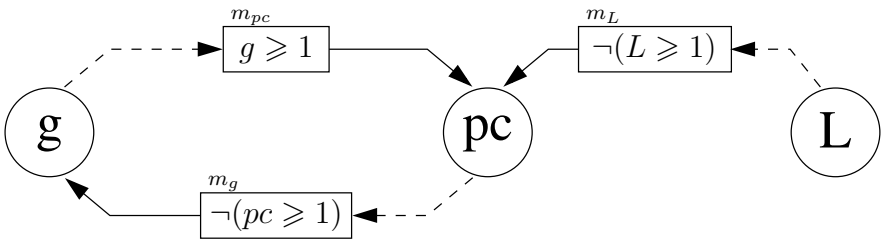

Figure 1: Interaction graph of the simplified gene regulatory network of the molecular circadian clock

Notation 1. ***[sign function]*** *The function* $sgn : \mathbb{R} \to \{-1, 0, 1\}$ *is defined by:*

$$sgn(x) = \begin{cases} \textit{-1} & \textit{if} \quad x < 0 \\ \textit{0} & \textit{if} \quad x = 0 \\ \textit{1} & \textit{if} \quad x > 0 \end{cases}$$

Definition 1. ***[Hybrid gene regulatory network]*** *A hybrid gene regulatory network (GRN for short) is a tuple $R = (V, M, E, \mathcal{C})$ where:*

- *V is a set whose elements are called* variables *of the network. Each variable is associated with a boundary $b_v \in \mathbb{N}^*$*
- *M is a set whose elements are called* multiplexes*. Each multiplex $m \in M$ is associated with a formula φ_m belonging to the language $\mathcal{L}$ inductively defined by:*
  - *If $v \in V$ and n is an integer such that $1 \leqslant n \leqslant b_v$, then $v \geqslant n$ is an atom of $\mathcal{L}$*
  - *If φ and ψ are two formulas of $\mathcal{L}$, then $\neg\varphi$, $(\varphi \vee \psi)$, $(\varphi \wedge \psi)$ and $(\varphi \Rightarrow \psi)$ also belong to $\mathcal{L}$*
- *E is a set of edges of the form $(m \to v) \in M \times V$.*
- *$\mathcal{C} = \{C_{v,\omega,n}\}$ is a family of real numbers indexed by the tuple (v, ω, n) where v, ω and n verify the three following conditions:*
  1. *$v \in V$*
  2. *ω is a subset of $R^-(v)$ where $R^-(v) = \{m \mid (m \to v) \in E\}$, that is ω is a set of predecessors of v.*
  3. *n is an integer such that $0 \leqslant n \leqslant b_v$*

  $C_{v,\omega,n}$ is called the celerity *of v for ω at the level n.*

Moreover, values of $C_{v,\omega,n}$ are constrained as in Figure 2. For each $v \in V$ and for each $\omega \subset R^-(v)$:

- *Either all celerities $C_{v,\omega,n}$ with $0 \leqslant n \leqslant b_v$ have the same non null sign,*
- *or there exists n_0 such that $C_{v,\omega,n_0} = 0$ and for all n such that $0 \leqslant n < n_0$, we have $sng(C_{v,\omega,n}) = 1$ and for all n such that $n_0 < n \leqslant b_v$, we have $sng(C_{v,\omega,n}) = -1$.*

In the classical Thomas' formalism, a parameter $K_{v,\omega}$ is a value such that $0 \leqslant K_{v,\omega} \leqslant b_v$. They represent the value toward which the variable v is attracted whereas celerities represent, in addition, the speed inside states. Celerities give more informations about the local dynamic of the model whereas the original Thomas' parameters only give global information. There exists a strong connexion between the original Thomas' parameters and our celerities (see Figure 2):

- If for all n, $C_{v,\omega,n}$ have a negative (resp. positive) sign, then $K_{v,\omega} = 0$ (resp. $K_{v,\omega} = b_v$)
- else $K_{v,\omega} = n_0$ (according to the previous definition)

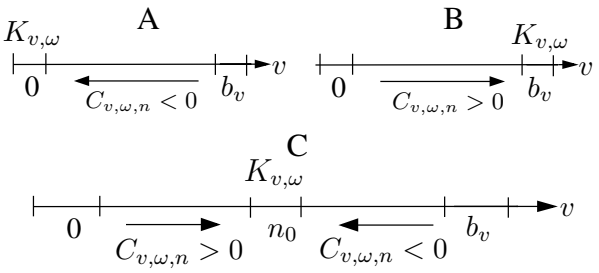

Figure 2: Signs of celerities according to the value of Thomas' parameter

Running example

Table 1 gives the network associated with Figure 1. This network has 8 qualitative states: 4 states $(g, pc) = (0,1), (0,1), (1,0)$ and $(1,1)$ in presence of light $(L = 1)$ and 4 other states in absence of light ($L = 0$).

V :	M :	E :	$\mathcal{C}$:		
g ($b_g = 1$)	m_{pc} : $\varphi_{m_{pc}}$	$(m_g \to g)$	$C_{g,\{\},0}$	$C_{pc,\{\},0}$	$C_{pc,\{m_L\},0}$
pc ($b_{pc} = 1$)	m_g : φ_{m_g}	$(m_{pc} \to pc)$	$C_{g,\{\},1}$	$C_{pc,\{\},1}$	$C_{pc,\{m_L\},0}$
L ($b_L = 1$)	m_L : φ_{m_L}	$(m_L \to pc)$	$C_{g,\{m_g\},0}$	$C_{pc,\{m_{pc}\},0}$	$C_{pc,\{m_L,m_{pc}\},0}$
	(see Figure 1)		$C_{g,\{m_g\},1}$	$C_{pc,\{m_{pc}\},1}$	$C_{pc,\{m_L,m_{pc}\},1}$

Table 1: Simplified GRN of the molecular circadian clock, following Figure 1.

2.2 Hybrid state and resources

Definition 2. ***[State of a GRN]*** *Let $R = (V, M, E, \mathcal{C})$ be a GRN. A* hybrid state *of R is a tuple $h = (\eta, \pi)$ where*

- *η is a function from V to $\mathbb{N}$ such that for all $v \in V$, $0 \leqslant \eta(v) \leqslant b_v$;*
  η is called the discrete state *of h.*
- *π is a function from V to the interval $[0,1]$ of real numbers,*
  π is called the fractional part *of h*

We denote H the set of hybrid states of R. When there is no ambiguity, we often use η and π without explicitly mentioning h.

The hybrid states combine two kinds of "states:" the discrete states (those of Thomas represented by η) and continuous positions inside the discrete states represented by π. As the width of a discrete state is 1, the domain of π is the continuous interval $[0,1]$.

Definition 3. ***[Resources]*** *Let $R = (V, M, E, \mathcal{C})$ be a GRN and let $v \in V$. The satisfaction relation $h \models \varphi$ (where $h = (\eta, \pi)$ is an hybrid state of R and φ a formula of $\mathcal{L}$) is inductively defined by :*

- *If φ is the atom $v \geqslant n$ with $n \in [1, \cdots, b_v]$, then $h \vDash \varphi$ iff $\eta(v) \geqslant n$*
- *If φ is of the form $\neg\psi$, then $h \vDash \varphi$ iff $h \nvDash \psi$*
- *If φ is of the form $\psi_1 \vee \psi_2$, then $h \vDash \varphi$ iff $h \vDash \psi_1$ or $h \vDash \psi_2$*
- *If φ is of the form $\psi_1 \wedge \psi_2$, then $h \vDash \varphi$ iff $h \vDash \neg(\neg\psi_1 \vee \neg\psi_2)$*
- *If φ is of the form $\psi_1 \Rightarrow \psi_2$, then $h \vDash \varphi$ iff $h \vDash (\psi_2 \vee \neg\psi_1)$.*

The set of resources of a variable v for a state h is defined by: $\rho(h, v) = \{m \in R^-(v) \mid h \vDash \varphi_m\}$, that is, the multiplexes predecessors of v whose formula is satisfied.

The notion of resources is important because it defines which celerity has to be considered in each discrete state: For our example, the celerity $C_{pc,\{m_{pc}\},1}$ (see Table 4.3) is used for the evolution of pc in the discrete states where $\eta(pc) = 1$ and the set of resources of pc is $\{m_{pc}\}$, that is where $\eta(g) \geqslant 1$ and $\eta(L) \geqslant 1$.

Remark 1. *The values of celerities are not proportional to the actual reaction speed in biology because we consider all discrete states with the same size (from 0 to 1) whereas, from a concentration point of view, the intervals of concentration can be of very different sizes.*

2.3 Hybrid trajectories

We now define the trajectories of the model, both inside a discrete state and at the crossing of thresholds (between two discrete states). We firstly define the touch delay, measuring the time necessary to touch the boundary of the current discrete interval.

Notation 2. ***[Touch delay]*** *Let $R = (V, M, E, \mathcal{C})$ be a GRN, v be a variable of V and $h = (\eta, \pi)$ be a hybrid state, we note $\delta_h(v)$ the* touch delay *of v in h for reaching the border of the discrete state. More precisely, δ_h is the function from V to $\mathbb{R}^+ \cup \{+\infty\}$ defined by:*

- *If $C_{v,\rho(v,\eta),\eta(v)} = 0$ then $\delta_h(v) = +\infty$*
- *If $C_{v,\rho(v,\eta),\eta(v)} > 0$ then $\delta_h(v) = \frac{1-\pi(v)}{C_{v,\rho(v,\eta),\eta(v)}}$*
- *If $C_{v,\rho(v,\eta),\eta(v)} < 0$ then $\delta_h(v) = \frac{\pi(v)}{|C_{v,\rho(v,\eta),\eta(v)}|}$*

If the celerity is null, the variable cannot evolve, thus the touch delay is infinite. Else, the touch delay depends on the associated celerity and the value $\pi(v)$.
$\delta_h(v) = 0$ means that the trajectory arrived on a border of the discrete state.

Let us notice that v may never reach its border: It is the case when another variable reaches its border before v (that is with a shorter δ_h).

Definition 4. ***[Black wall and boundary]*** *Let $R = (V, M, E, C)$ be a GRN, let $v \in V$ be a variable, let $h = (\eta, \pi)$ and $h' = (\eta', \pi')$ be two hybrid states such that η and η' are neighbour states w.r.t. v, that is $\eta'(v) = \eta(v) + sgn(C_{v,\rho(v,\eta),\eta(v)})$ and $\eta'(u) = \eta(u)$ for all $u \neq v$.*

1. *v is said on a* black wall *if the two following conditions are satisfied:*
   - $\delta_h(v) = 0$
   - $sgn(C_{v,\rho(v,\eta),\eta(v)}) \times sgn(C_{v,\rho(v,\eta'),\eta'(v)}) = -1$
2. *v is said on a* boundary *if the two following conditions are satisfied:*
   - $\delta_h(v) = 0$
   - *At least one of the following conditions holds:*
     - $C_{v,\rho(v,\eta),\eta(v)} < 0$ *and* $\eta(v) = 0$
     - $C_{v,\rho(v,\eta),\eta(v)} > 0$ *and* $\eta(v) = b_v$.

We note $slide(h)$ the set of variables that are either on a black wall or on a boundary.

We can remark that for each hybrid state, the continuous component takes its values in the interval $[0, 1]$, leading to a sort of a "double threshold" between two neighbour discrete states, as $h(v) = (n, 1)$ differs from $h(v) = (n + 1, 0)$. The behaviour of the system will use this "double threshold" for sliding states.

For example, it becomes possible to slide on a "black wall" (Definition 4.1). The trajectories from one of these discrete states do not cross the threshold (because on the opposite side, the celerities make impossible an entering trajectory). See Figure 3A.

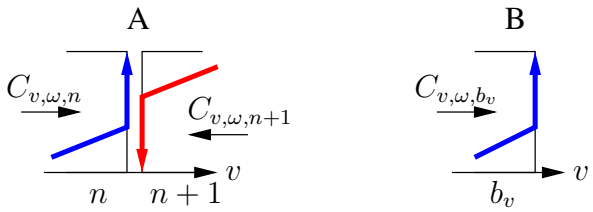

Figure 3: (A) Example of a black wall. (B) Example of a boundary

Also, in a discrete state such that $\eta(v) = b_v$ (resp. $\eta(v) = 0$) where $C_{v,\dots} > 0$ (resp. $C_{v,\dots} < 0$), the variable v cannot cross the boundary (there is no state on the other side). Then, other variables can allow the trajectory to slide on the boundary. See Figure 3B.

Definition 5. ***[Knocking variables]*** *Let $R = (V, M, E, C)$ be a GRN and $h = (\eta, \pi)$ be a hybrid state, the set of* knocking variables *is defined by :*

$first(h) = \{v \in V \setminus slide(h) \mid \delta_h(v) < +\infty$ *and* $\forall u \in V \setminus slide(h),\ \delta_h(u) \geqslant \delta_h(v)\}$

The set $first(h)$ represents the set of variables whose qualitative value can change first. If the variable is on a sliding wall, it cannot evolve as long as other variables do not change. Similarly, if the celerity of a variable v in the current state is null, its qualitative value cannot change because of its infinite delay.

Definition 6. ***[Hybrid state space]*** *Let $R = (V, M, E, C)$ be a GRN, we note $\mathcal{R} = (H, T)$ the* hybrid state space *of R where H is the set of hybrid states and T is the set of* transitions*: There exists a transition from (η, π) to (η', π') iff there exists a variable $v \in first(h)$ such that*

1. *Either $\delta_h(v) \neq 0$ and*
   - *(i)* $\eta' = \eta$
   - *(ii)* $\pi'(v) = \frac{1+sgn(C_{v,\rho(v,\eta),\eta(v)})}{2}$ *for all $v' \in first(h)$ (i.e. 0 if $C_{v,\rho(v,\eta),\eta(v)} < 0$ and 1 if $C_{v,\rho(v,\eta),\eta(v)} > 0$).*
   - *(iii) For all variables $u \neq v$, if $u \notin slide(h)$ then $\pi'(u) = \pi(u) + \delta_h(v) \times C_{u,\rho(u,\eta),\eta(u)}$, else $\pi'(u) = \pi(u)$.*
2. *or $\delta_h(v) = 0$ and*
   - *(i)* $\eta'(v) = \eta(v) + sgn(C_{u,\rho(v,\eta),\eta(v)})$
   - *(ii)* $\pi'(v) = \frac{1-sgn(C_{v,\rho(v,\eta),\eta(v)})}{2}$ *(i.e. 0 if $C_{v,\rho(v,\eta),\eta(v)} > 0$ and 1 if $C_{v,\rho(v,\eta),\eta(v)} < 0$).*
   - *(iii) For all variables $u \neq v$, $\eta'(u) = \eta(u)$ and $\pi'(u) = \pi(u)$*

There are two different kinds of transitions:

1. Inside a discrete state: The idea is to determine a next hybrid state which could give rise to a qualitative change. Thus, from a hybrid state, one has to determine the variables which first reaches the border of the discrete state. The resulting hybrid state is then the one where the fractional part of v is equal to 0 or 1 (see $1.ii$), and other variables are changed accordingly. Inside a given discrete state, all trajectories of the hypercube are parallel ones because all hybrid states have the same celerities.
2. Between two discrete states: If the system cannot evolve anymore within the current discrete state, the trajectory goes through a border: The discrete part is computed according to the sign of the celerity (see $2.i$) and the fractional part is either 1 or 0 according to the sign of celerities (see $2.ii$). Other variables are not changed.

This semantics has been inspired by the trajectories produced by the usual stepwise linear ordinary differential equation systems [20]. In the neighbourhood of a black wall, the trajectories on one side of the threshold are issued from the differential system of *this* side. In other words, even if the trajectory remains very close to the threshold: the evolution depends on the domain from which the trajectory comes. This is why in our semantics, all slidings on a black wall, take place inside the discrete state from which the trajectory comes.

Running example

To illustrate the transitions, let us consider the hybrid state d of Figure 12-B. d is of the form $d = ((1, 0), (0, d_y))$: the discrete state is $(\eta(g) = 1, \eta(pc) = 0)$ and

the fractional part is $(\pi(g) = 0, \pi(pc) = d_y)$ where $0 < d_y < 1$. In this discrete state, both celerities are positive. In the figure, we see that $\delta_d(g) < \delta_d(pc)$. So $first(d) = \{g\}$. Thus, the trajectory reaches the boundary of g on which g is able to slide (hybrid state d_1 in the figure). The rest of the trajectory follows the same reasoning according to Definition 6: It slides along the boundary according to the celerity of pc and reaches state f. The trajectory crosses the pc threshold and enters into the next discrete state. In the next discrete state, we have $\delta_a(g) > \delta_a(pc)$, thus the boundary of pc is first reached. The trajectory slides on the boundary of pc according to the celerity of g to reach the threshold of g and finally reach the hybrid state b.

3 The HyMBioNet software

The main difficulty when modelling GRN lies in the parameter identification. Model checking has been widely used in purely discrete frameworks to select parameters allowing the model to fulfil all the known biological behaviours [7]. However, in hybrid formalisms, this method leads to very complex procedures [23]. In practice, we currently use CTL to express known biological behaviours and we use model checking *via* SMBioNet [7] to select parameters of the purely discrete Thomas' model. We then automatically deduce the sign of celerities of our hybrid model (see Section 2.1). To go further, we choose to perform simulations within the hybrid model. In this aim, we developed a user-friendly software platform to generate and to simulate a network in order to confront the model with biological expertise. The HyMBioNet platform (`http://i3s.unice.fr/~enee/HyMBioNet/`) consists in two tools: The first one allows the construction of a GRN through a web interface and generates the code of a simulator in the NetLogo language [25]. This simulator can then be used *ad libitum*. We describe these two tools in this section.

3.1 The HyMBioNet web interface

In order to build a GRN, we first have to list the genes and we also allow the use of *zeitgeber*. A zeitgeber is an external variable that influences upon gene(s); such a variable behaves independently of the rest of the network. For example, the night and day alternance is a zeitgeber for a circadian clock gene network.

Adding genes and zeitgebers

Figure 4 shows the main web application. The user is repeatedly invited to fill a gene name, to indicate the associated boundary and then to press the "Add Gene" button. Zeitgebers can be added thanks to the same mechanism in the "Add new zeitgeber" filling zone.

Adding multiplexes

When the genes and the zeitgebers have been given, the user is invited to describe the multiplexes. Figure 5 gives the description step by step of how to create the multiplex Ml, i.e., the multiplex that explains the influence of the "Light" zeitgeber on pc in our model. First, the name of the multiplex is filled in the "Rule name" field (Figure 5-A); note that this field appears when there is at least one gene in the network. Then

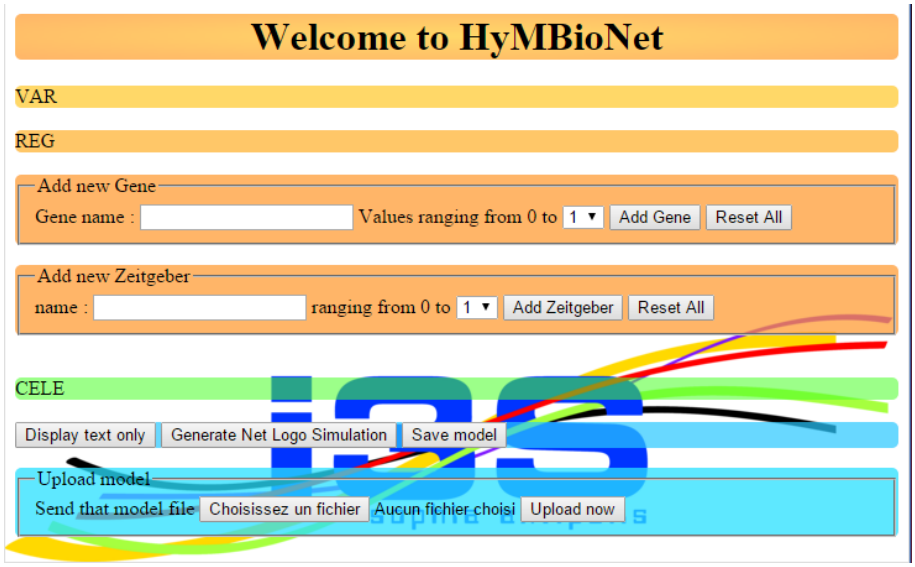

Figure 4: HyMBioNet web interface

the user is invited to write the formula associated with this multiplex thanks to a user friendly interface that prevents errors by guiding the user along the syntactic tree of the formula (5-B). Here the formula of the multiplex Ml is $\neg(L \geq 1)$ and it has the gene "pc" as target. In step 5-C, the user has chosen L as the variable that controls the multiplex Ml. In step 5-D, the user selects the comparator "$\geqslant$". Next, (s)he selects the value of L used for the comparison: only the possible values corresponding to L are shown (step 5-E). As the formula of this multiplex contains a negation, the "Not ?" checkbox has to be checked and then the "Not or not Not ?" button has to be pressed (see 5-F). To finish multiplex description, the target of the multiplex is checked (here the variable pc) and the button "Update Rule Targets" is pressed: the final multiplex is displayed in Figure 5-G.

Automatically added Celerities

Whereas genes, zeitgebers and multiplexes are acquainted by the user, celerities described in Section 4 are automatically listed by the application. Figure 6 shows the "display text" version of the simple mammalian circadian model. The number of celerities associated with a gene depends on the number of multiplexes that regulate this gene and also on the qualitative levels of this gene (see Definition 1). There is a celerity for each subset of regulations (if g is regulated by n multiplexes, there are 2^n possible subsets) and for each qualitative level. All celerities are produced regarding multiplex targets that are described in the "REG" part.

For example, pc is regulated by multiplexes Mpc and Ml. There are 4 possible subsets of regulators: $\varnothing$, $\{Mpc\}$, $\{Ml\}$ and $\{Mpc, Ml\}$. This gives rise to the celerities `C_pc[]`, `C_pc[Mpc]`, `C_pc[Ml]` and `C_pc[Mpc,Ml]`, but pc can take two

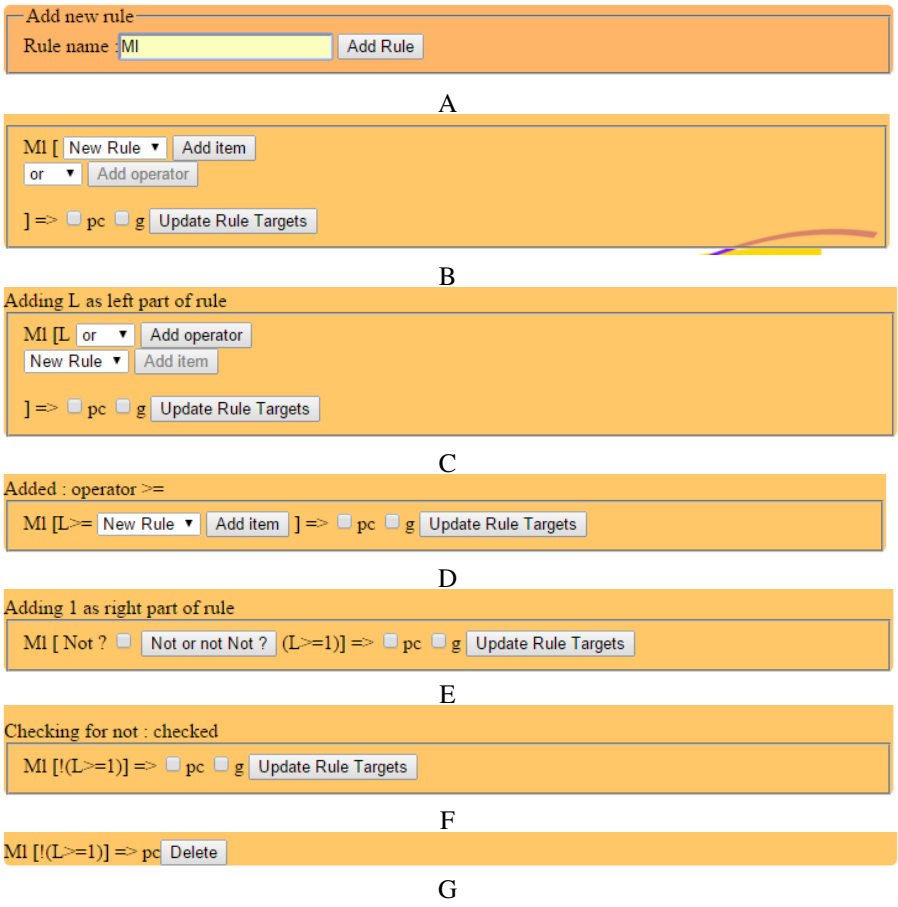

Figure 5: Interface for creating a multiplex

distinct qualitative levels, so we get the 8 celerities of Figure 6 (see green zone).

Features

We added the possibility to save and upload a model. This is very useful to test different options. As a second enhancement, we offer to delete useless celerities (that are never used because of the unsatifiability of the associated multiplex formulas) in order to produce a lighter simulation.

Export your simulation

Lastly, when modelling is complete, one can export the corresponding NetLogo simulator with the "Generate Net Logo Simulation" button.

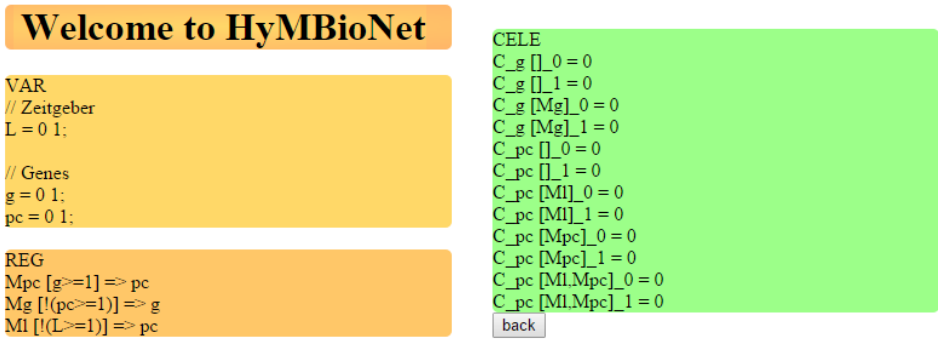

Figure 6: Simple model of the mammalian circadian clock

3.2 NetLogo simulation

The NetLogo simulation is shown in Figure 7. The black board is where the GRN is displayed and animated.

On the left side, there are three buttons. One to "Setup" a simulation, the second to make a simulation "Step by step" and the third to make a "Loop" simulation. While running, plots are automatically updated with data, for each variable: The level of each variable is represented by the algebraic sum of the current qualitative level and the current position inside this discrete state. Plots can be exported in CSV format thanks to export buttons.

On the right side of the central black board, it is possible to change the number of simulation steps per hour: if this slider is set to 1, there is a unique simulation step for each hour, and if it is set to 60, each step of simulation corresponds to 1 minute between two clock ticks. Under this slider, three other sliders allow the user to set the initial gene / zeitgeber values. The current value is shown on the left of the slider.

Zeitgeber language description

As zeitgebers are specific variables that are able to influence the network but are not influenced by it, we propose a small language to describe the time evolution of zeitgebers.

The Language is the following:

- $formula \ ::== \ [daylist]$
- $daylist \ ::== \ day \mid day \ daylist$
- $day \ ::== \ [pair\_value\_list][how\_many\_times]$
- $pair\_value\_list \ ::== \ pair\_value \mid pair\_value \ pair\_value\_list$
- $pair\_value \ ::== \ [hours \ \ value]$

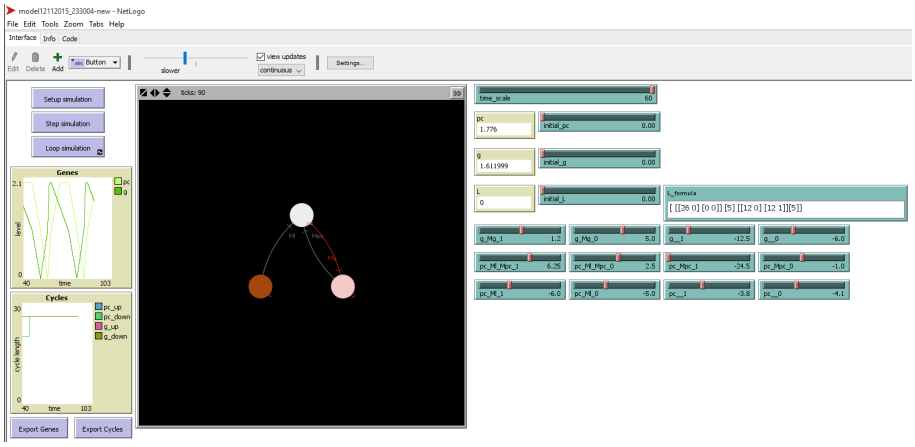

Figure 7: Netlogo Simulation

where $hours$ is the number of hours the zeitgeber will stay in the specified discrete $value$ and how_many_times is the number of times the previous described cycle is repeated. For example, in Figure 7, the expression `[[[12 0] [12 1]][1]]` indicates that the zeitgeber will be at the discrete level 0 for 12 hours, then it will change to discrete value 1 for the next 12 hours and finally that cycle is not repeated. When the cycle is finished, i.e., the day has passed here, the system will restart that cycle from the beginning.

Fixing celerities

The simulator manages delays instead of celerities (delays are easier to handle). Because the length of each qualitative interval is one, the mandatory delay to cross an interval is equal to $\frac{1}{celerity}$. Thanks to sliders varying in $[-25; 25]$ with a 0.1 increment, one can fix each delay of the described model. Delays are named in the same manner than celerities. The settings corresponding to celerities of Table 4.3 are shown in Figure 8.

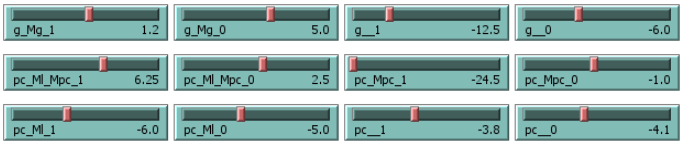

Figure 8: Chosen delays

Running example

After delays are fixed, the simulation must be "setup" in order to display genes, zeitgeber and multiplexes (see Figure 9). Simulation is launched using the "Loop simu-

lation" button while a step by "step simulation" button is available to slowly observe transitions.

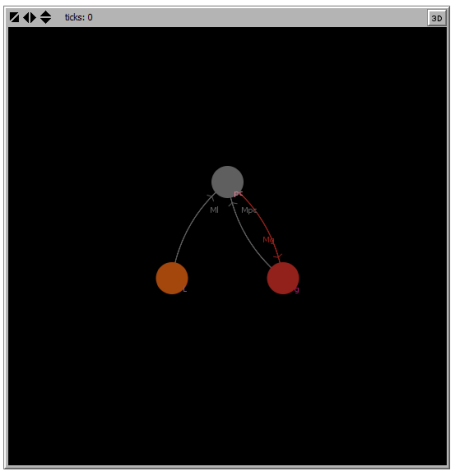

Figure 9: Main simulator view after setup

Figure 10-A shows that the length of the mammalian circadian cycle is, as expected, about 26 hours in constant dark. In Figure 10-B, the cycle is 24 hours when exposed to a 12h/12h alternation of dark and light. In that case, g gene does not reach the 0 sliding wall.

To produce those plots, the formula controlling the time evolution of the zeitgeber is: `[[[26 0][0 0][5][[12 0][12 1]][5]]`. Five 12h/12h alternations of dark/light follow five cycles of 26 hours in constant dark.

Drawback

If a network has a large number of parameters, sliders will not all fit into the screen space and will only be accessible *via* scroll bars.

4 Identification of celerities

As usual, a key point of the modelling process is the parameters identification. This identification has to be done taking into account the known behaviours of the biological system.

On our example, the crucial and the simplest property that the model has to exhibit is the following: the circadian clock has sustained oscillation, even if no zeitgeber controls the oscillation. Of course we can make a lot of simulations using HyMBioNet in order to get an intuition about the celerities allowing the model to behave as expected. However, we would like to provide a full analysis in order to build constraints on celerities making possible a sustained oscillation in constant dark (in the plane $L = 0$). Following the preliminary model of the circadian clock [9], we deduce the

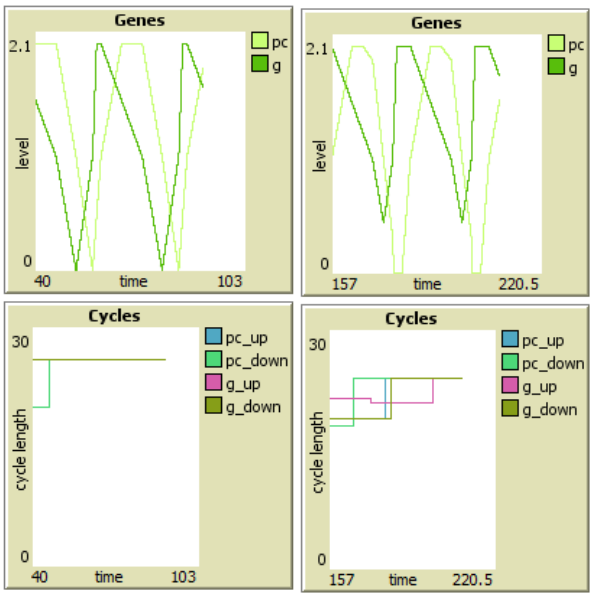

A B

Figure 10: Circadian cycle simulation

sign of all celerities and then the direction of the rotation of the cycle: in counter-clockwise direction ((0,0)→(1,0)→(1,1)→(0,1)→(0,0)), see Figure 12.

In this section, we firstly prove that in order to exhibit a unique attractive limit cycle, the limit cycle has to slide on a boundary. In Section 4.2, we use the previous property to build a relationship between the different slopes of the cyclic trajectory. Finally, Section 4.3 uses the known period in order to constrain celerities.

4.1 Using 2D remarkable properties

Notation 3. *Let us note respectively* $slope_{00}, slope_{01}, slope_{10}, slope_{11} \in \mathbb{R}_+^*$ *the "slope" of trajectories inside each discrete state* $(0,0), (0,1), (1,0), (1,1)$.

- *in* $(0,0)$, $slope_{00} = \frac{-C_{pc,\{m_{pcl}\},0}}{C_{g,\{m_g\},0}} > 0$
- *in* $(0,1)$, $slope_{01} = \frac{C_{pc,\{m_{pcl}\},1}}{C_{g,\varnothing,0}} > 0$
- *in* $(1,0)$, $slope_{10} = \frac{C_{pc,\{m_{pcl},m_{pcg}\},0}}{C_{g,\{m_g\},1}} > 0$
- *in* $(1,1)$, $slope_{11} = \frac{C_{pc,\{m_{pcl},m_{pcg}\},1}}{-C_{g,\varnothing,1}} > 0$

Let us remark that for geometrical facility, we take the absolute value of the mathematical slopes.

Proposition 1. *Let* $R = (V, M, E, \mathcal{C})$ *be a GRN where* $|V| = 2$ *and the boundaries of both variables are equal to 1. There exists a unique attractive limit cycle if and only if there exists a cyclic trajectory that slides on at least one external boundary.*

Proof. Necessary condition: If there is no place where the cyclic trajectory slides, then because all slopes are constant in each of the four discrete states, there would be an infinity of different cyclic parallel trajectories (Figure 11-A):

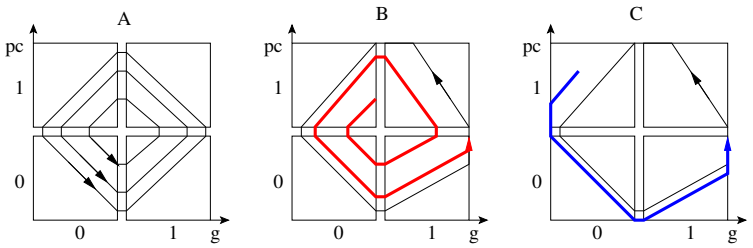

Figure 11: (A) State graph with an infinity of cyclic trajectories. (B) State graph with trajectory inside cycle. (C) State graph with external trajectory

Thus, there is at least one sliding.
Sufficient condition: If there exists a cyclic trajectory that slides on an external boundary then it is unique and attractive because:

- For any hybrid state inside the cycle, its trajectory after exactly one rotation (Figure 11-B) will lead to a state that is strictly closer to the surrounding cycle (divergent red "spiral"). The sequence of such points after n rotations will cross the limit cycle.
- Similarly, for any hybrid state outside the cycle, its (blue) trajectory will necessary stay outside the cycle because, in 2D, trajectories never cross each other. Consequently, its trajectory will necessary slide where the limit cycle slides, and join the limit cycle after at most one rotation (Figure 11-C).

□

4.2 Constraints on the slopes of the cyclic trajectory

Here we would like to build some constraints on celerities in order to facilitate the choice of "valuable" celerities. The high synthesis rate of PER and CRY proteins leads to an accumulation of PER-CRY complexes in the cytoplasm. This accumulation induces a fast crossing of complexes into the nucleus, so, a saturation of the nucleus by PER-CRY complex [9]. According to these informations, we impose 2 slidings in our model.

- The cyclic trajectory slides in the discrete state $(1, 0)$ for the maximal rate of the transcription of clock genes and
- it also slides in $(1, 1)$ for the saturation of PER-CRY complex in the nucleus.

Figure 12-B represents the expected trajectory in constant dark conditions.

As we have fixed the slidings on states $(1, 0)$ and $(1, 1)$, we know that the first hybrid state of the cyclic trajectory in $(1, 1)$ has $(1, 0)$ for fractional coordinates(see Figure 12-B). To have a sliding in the state $(1, 1)$, pc must touch its boundary before g.

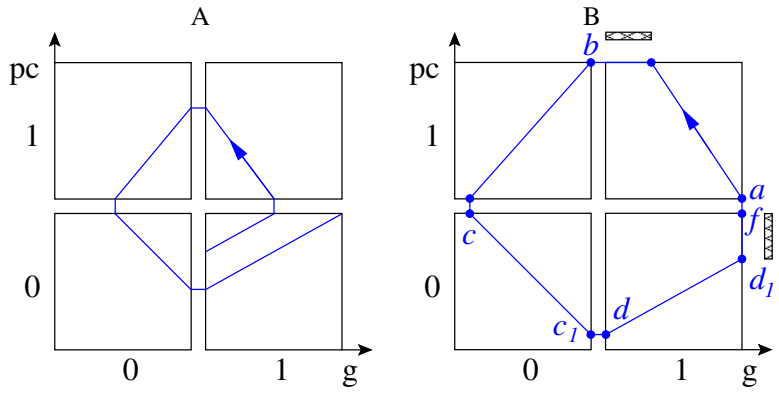

Figure 12: Trajectories of the simplified circadian clock model in constant dark. (A) A trajectory with an initial state inside the cycle. (B) The limit cycle.

1. Constraint for the discrete state $(1,1)$: The trajectory must slide on the threshold of pc, so $slope_{11} > 1$.
2. Constraints on $(0,1)$. In this discrete state, the trajectory begins at the hybrid state b. As the trajectory does not reach the boundary of g, pc must reach its threshold before g. Thus, we have $slope_{01} \geqslant 1$.
3. Constraints on $(0,0)$. The fractional coordinates of the hybrid state c are $(-slope_{01}, 1)$ and those of the state c_1 are $(0, -slope_{01} \times slope_{00})$. This leads to the constraints $slope_{00} \times slope_{01} \leqslant 1$.
4. Constraints on $(1,0)$. The fractional coordinates of the hybrid state d are $(0, -slope_{00} \times slope_{01})$. As this discrete state contains a sliding on the boundary of g, the trajectory must reach it before the threshold of pc. This leads to the constraints $slope_{00} \times slope_{01} > slope_{10}$.

Among the constraints, we keep the first constraint $slope_{11} > 1$ for the sliding inside the discrete state $(1,1)$ and the last constraint $slope_{00} \times slope_{01} > slope_{10}$ for the sliding inside the discrete state $(1,0)$ depending on the previous states $(0,0)$ and $(0,1)$.

4.3 Using the length of the period of the circadian clock in constant dark

Notation 4. *Let us denote by* $\delta^g_{00}, \delta^{pc}_{01}, \delta^{pc}_{10}, \delta^g_{11} \in \mathbb{R}^*_+$ *the times to cross each states* $(0,0), (0,1), (1,0), (1,1)$ *respectively.*

These crossing delays depend on the only variable that can change its qualitative value and its celerity. For example, in the state $(0,0)$, only the variable pc can evolve because g goes toward its boundary and slides on it. Thus, the only delay to be taken into account is the delay of pc.

Without the zeitgeber, the clock have a period between 22 and 25 hours depending of the tissue [26]. Here, we voluntarily chose a longer period of 26 hours to an easier

observation of the effect of zeitgeber (the light) on the synchronisation. Thus we impose: $\delta^g_{00} + \delta^{pc}_{10} + \delta^g_{11} + \delta^{pc}_{01} = 26$.

- For the discrete state $(1,1)$, $\delta^g_{11} = \frac{1}{C_{g,\rho(a,g),1}}$ because the crossing distance of g is equal to 1.
- For the discrete state $(0,1)$, for the same reasons we have $\delta^{pc}_{01} = \frac{1}{C_{pc,\rho(c,pc),1}}$.
- In $(0,0)$, the crossing distance is equals to $slope_{01}$. Thus, we have $\delta^g_{00} = \frac{slope_{01}}{C_{g,\rho(d,g),0}}$.
- In $(1,0)$, the crossing distance of pc equals to $slope_{00} \times slope_{01}$, so we have $\delta^{pc}_{10} = \frac{slope_{00} \times slope_{01}}{C_{pc,\rho(e,pc),0}}$.

At the end, to have a cycle in constant dark, celerities must satisfy the following constraint :

- $slope_{10} > slope_{00} \times slope_{01}$
- $slope_{11} > 1$
- $\frac{1}{C_{g,\rho(a,g),1}} + \frac{1}{C_{pc,\rho(c,pc),1}} + \frac{slope_{01}}{C_{g,\rho(d,g),0}} + \frac{slope_{00} \times slope_{01}}{C_{pc,\rho(e,pc),0}} = 26$

The Table 4.3 contains the chosen celerities to make the simulations of Section 5.

g			pc		
$C_{g,\{\},0}$	=	-0.167	$C_{pc,\{\},0}$	=	-0.244
$C_{g,\{\},1}$	=	-0.08	$C_{pc,\{\},1}$	=	-0.262
$C_{g,\{m_g\},0}$	=	0.2	$C_{pc,\{m_{pc}\},0}$	=	-1.0
$C_{g,\{m_g\},1}$	=	0.8	$C_{pc,\{m_{pc}\},1}$	=	-0.041
			$C_{pc,\{m_L\},0}$	=	-0.2
			$C_{pc,\{m_L\},1}$	=	-0.167
			$C_{pc,\{m_L,m_{pc}\},0}$	=	0.4
			$C_{pc,\{m_L,m_{pc}\},1}$	=	0.16

Table 2: Chosen parameters values according to constrains determined in Section 4.

5 Some results

In the sequel, the couple $(\eta(v), \pi(v))$ where (η, π) is a hybrid state, describes the qualitative level and the fractional part of variable v, and such a couple is represented by the algebric sum $\eta(v) + \pi(v)$. Thus the real number 1.5 represents the couple $(1, 0.5)$. However the real number 2.0 represents both couples $(1, 1.0)$ and $(2, 0.0)$. In other words, two points on both sides of a threshold are merged.

In Figures 13, 14 and 15, red (resp. blue) curves represent the evolution of pc (resp. g), whereas the grey zones correspond to the dark phases ($L = 0$). The dashed line represents the threshold of each variable. Used parameters are those of Table 4.3.

5.1 Light as zeitgeber: constant dark vs. equinox

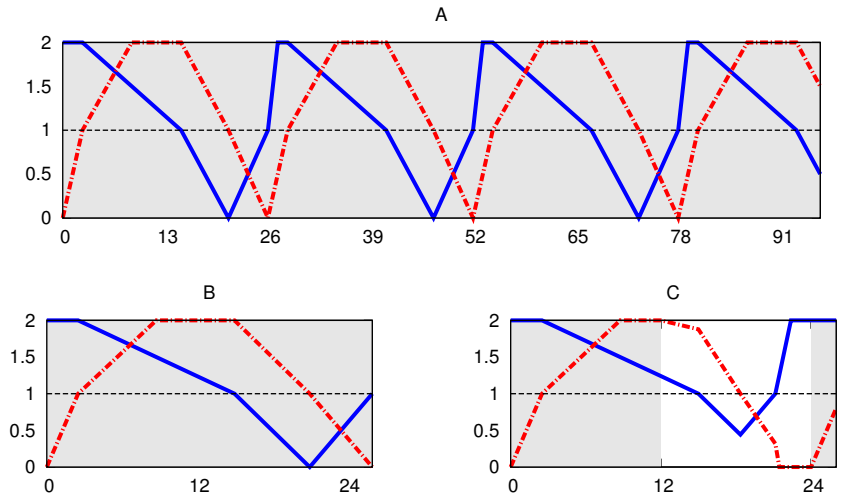

Figure 13: (A) Full simulation in constant dark (B) Zoom on a single cycle in constant dark (C) Simulation of the model submitted to a 12h/12h oscillations of dark and light.

The Figure 13-A represents the simulation in constant dark conditions. The sustained oscillations have a 26-hours period. Each sliding imposed in the previous section is observable in the figure: It is represented by the horizontal segments where $g = 2$ (or where $pc = 2$). Figure 13-B is a zoom on a single cycle of Figure 13-A. Figure 13-C, shows the behaviour of the model with the adding of the dark/light oscillation with 12 hours of light and 12 hours of dark (equinox). During the light phase, the decrease is stronger than during the dark phase (B). This disruption allows the model to reach, before the end of the cycle (between 23 and 24 hours), a state where neither g (blue) nor pc (red) can move anymore. We call it the "waiting state" because this state remains stable until the next dark phase starts and allows the system to synchronise to the stable period imposed by the zeitgeber.

5.2 Circadian clock and seasons

Figure 14 shows the behaviour of the model submitted to different seasonal conditions. In conditions A and B, corresponding respectively to summer and winter, in temperate zone, the amplitude of the curves of g and pc changes slightly but the system is able to maintain a periodic behaviour of 24 hours. The waiting state plays the role of a "buffer" to make the system robust to the dark/light alternation disruption.

- In extreme winter condition (D), the waiting state disappears and the end of the cycle happens after 24 hours. Thus, the system tends toward a 26 hours period as in constant dark period: The light phase is not long enough to synchronize the circadian clock with a 24-hours period.

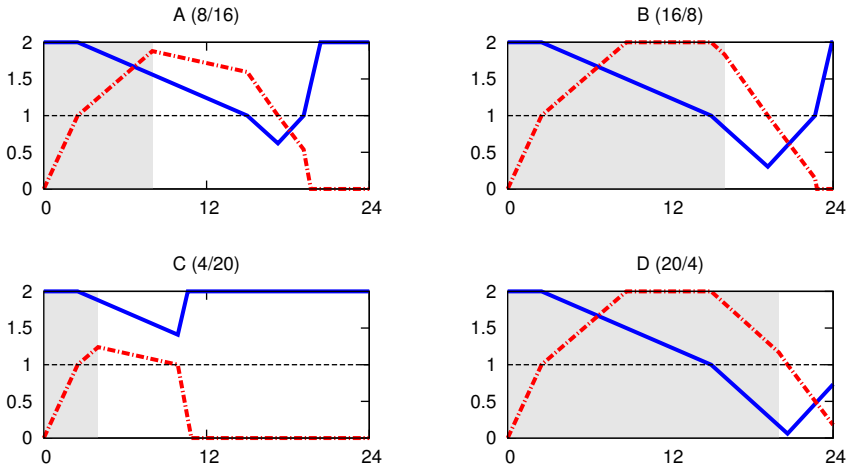

Figure 14: Simulations of the model submitted to alternation of dark and light. (A) 8 hours dark followed by 16 hours light. (B) 16 hours dark followed by 8 hours light (C) 4 hours dark followed by 20 hours light (D) 20 hours dark followed by 4 hours light.

- In extreme summer condition (C), the amplitude of the curves decrease as in B, but this time, g does not cross its threshold anymore. The system oscillates between the discrete states $(1, 0)$ and $(1, 1)$ (for (g, pc)) thus the variable g is not repressed anymore.

Schmal *et al.* [18] present a theoretical study of seasonality in which they focus on entrainment of the circadian clock under different conditions. In particular, they present a "Arnold's onion" which show the entrainment zone of the circadian clock according to the period and the photoperiod (percentage of dark in 24 hours). It is worth mentioning that our simulations with a remarkably simple model (constant dark condition, summer and winter conditions) are all within the entrainment zone of the onion. At the opposite, the conditions in which the photoperiod is extreme (4 and 20) are not within the onion.

5.3 Jet lags

Figure 15 shows the behaviour of the model during a 8 hours jet lag. Figures 15-A and 15-C represent the behaviour of the model when the circadian clock is affected by a jet lag toward West. Figures 15-B and 15-D represent its behaviours for a jet lag toward East. Cycles before 48 hours and after 104 (for A and C) and 88 (for B and D) are not represented because they exhibit the same behaviour as in the case of the 12/12 dark/light oscillations of Figure 13-C.

- For light phase elongation (A), the first 24 hours are the same as under the equinox condition. In the next 8 hours, the system stays in the waiting state until the next dark phase.

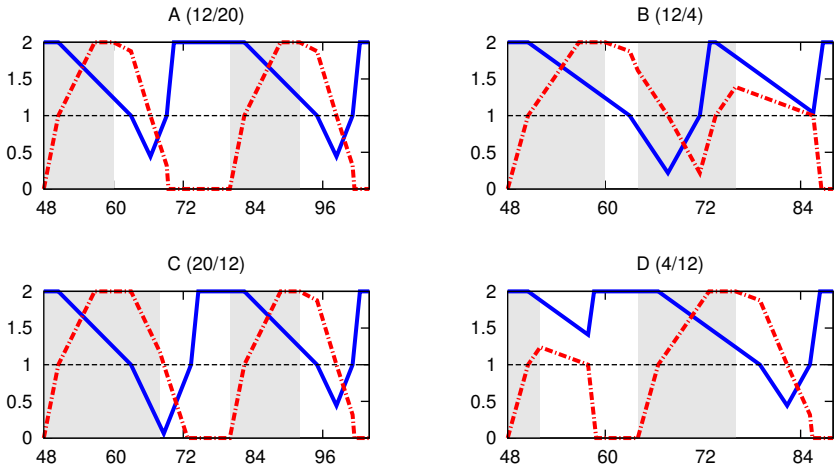

Figure 15: Simulations with 8-hours jet lags. (A) Jet lag toward West during the day: The light duration is increased from 12 to 20 hours. (B) Jet lag toward East during the day: The light duration is decreased from 12 to 4 hours. (C) Jet lag toward West during the night: The dark duration is increased from 12 to 20 hours. (D) Jet lag toward East during the night: The dark duration is decreased from 12 to 4 hours. Each simulation is preceded and followed by two 12h dark and 12h light cycles. The windows contain the cycle of the jet lag and the next one.

- For the dark phase elongation (C), the first cycle is the same as under the constant dark condition (Figure 13-B) where the period is 26 hours, but the light phase is sufficient to allow the system to reach the waiting state and thus to ensure the synchronisation of the clock to a 24-hours period.

Nevertheless, the jet lag toward East has more adverse effects.

- When the light phase is shortened (Figure 15-B), it can be not long enough to synchronize the clock in the first cycle. Moreover, the shift of the system causes a cycle stop in the next day (the blue curve does not go under 1).
- When the dark phase is shortened (Figure 15-D), one observes the same kind of stop in the first cycle but it resumes the next day.

Despite the simplicity of our model, it reproduces notably a lot of real behaviours of the mammalian circadian clock.

6 Conclusion

The hybrid formalism presented in this chapter is inspired by the simplicity of the Thomas' modelling framework. The celerities of this modelling framework give the direction and the evolution speed of the system within each discrete state. This formalism mixes the qualitative trajectories as in the Thomas' formalism, with a notion

of delays of transitions from a state to another. Such data (delays between 2 distant states) is easily measurable during an experiment.

Proof of concept of our hybrid framework is done through a tiny model of the mammalian circadian clock. The celerities have been identified according to biological behaviours. We first identified constraints on celerities owing to a limit cycle of known period. This method is nevertheless dedicated to small dimensions, so our future work will be dedicated to extensions of the computer aided identification methods already available for the discrete case.

We equipped this new hybrid framework with a simulator generator. This generator allows biologist to generate their own models and make their own *in silico* experiments. This program assists the user to create the network by a web interface, a NetLogo file is then generated and can be executed to observe the behaviour of the model. This interface allows one to choose zeitgebers behaviour (in our example, a scenario for alternations of light and dark) and to modify celerities in real time. Moreover, it shows the level of each variables at each step and the evolution of periods.

Despite its simplicity, our circadian clock model provides interesting behaviours: In constant dark, in 12h/12h alternations of light and dark, in different seasons (modification of the light proportion within a 24-hours period) and when jet lags (modification of one cycle) occur. In constant dark and dark/light alternation conditions, the simulations are very close to the observations. This adaptation faculty is due to the presence of a stable hybrid state (waiting state) allowing the synchronization of the system with the cycle imposed by the external light/dark alternation.

In order to go further on more elaborated models, we have to facilitate the identification of celerities by establishing heuristics able to construct constraints on celerities which have to be satisfied to allow the model to behave as expected. The Hoare logic [4] seems to be a promising first approach.

References

[1] R. Alur, C. Belta, F. Ivančić, V. Kumar, M. Mintz, G. J. Pappas, H. Rubin, and J. Schug. Hybrid modeling and simulation of biomolecular networks. In *Hybrid Systems: Computation and Control*, pages 19–32. Springer, 2001.

[2] D. Barik, W. T. Baumann, M. R. Paul, B. Novak, and J. J. Tyson. A model of yeast cell-cycle regulation based on multisite phosphorylation. *Molecular Systems Biology*, 6(1):405, 2010.

[3] S. Becker-Weimann, J. Wolf, H. Herzel, and A. Kramer. Modeling feedback loops of the mammalian circadian oscillator. *Biophysical Journal*, 87(5):3023 – 3034, 2004.

[4] J. Behaegel, J.-P. Comet, G. Bernot, E. Cornillon, and F. Delaunay. A hybrid model of cell cycle in mammals. *Journal of Bioinformatics and Computational Biology*, 14(1), 2016, In Press.

[5] W. J. Belden, J. J. Loros, and J. C. Dunlap. Clock leaves its mark on histones. *Trends in Biochemical Sciences*, 31(11):610–613, 2006.

[6] G. Bernot and J.-P. Comet. On the use of temporal formal logic to model gene regulatory networks. In *Computational Intelligence Methods for Bioinformatics and Biostatistics*, pages 112–138. Springer, 2010.

[7] G. Bernot, J.-P. Comet, A. Richard, and J. Guespin. Application of formal methods to biological regulatory networks: extending thomas' asynchronous logical approach with temporal logic. *Journal of theoretical biology*, 229(3):339–347, 2004.

[8] K. Bozek, A. Relógio, S. M. Kielbasa, M. Heine, C. Dame, A. Kramer, and H. Herzel. Regulation of clock-controlled genes in mammals. *PLoS One*, 4(3):e4882, 2009.

[9] J.-P. Comet, G. Bernot, A. Das, F. Diener, M. C., and A. Cessieux. *Proc. of the Evry Spring school on Modelling complex biological systems in the context of genomics*, chapter Simplified models for the mammalian circadian clock, pages 85–106. EDP Sciences, 2012.

[10] J.-P. Comet, J. Fromentin, G. Bernot, and O. Roux. A formal model for gene regulatory networks with time delays. In *1st Intl. Conf. on Computational Systems-Biology and Bioinformatics*, pages 1–13. Springer, 2010.

[11] C. Crosio, N. Cermakian, C. D. Allis, and P. Sassone-Corsi. Light induces chromatin modification in cells of the mammalian circadian clock. *Nature neuroscience*, 3(12):1241–1247, 2000.

[12] D. B. Forger and C. S. Peskin. A detailed predictive model of the mammalian circadian clock. *PNAS*, 100(25):14806–14811, 2003.

[13] C. Gérard and A. Goldbeter. Temporal self-organization of the cyclin/cdk network driving the mammalian cell cycle. *PNAS*, 106(51):21643–21648, 2009.

[14] N. R. Glass. Computer analysis of predation energetics in the largemouth bass. *Systems analysis and simulation in ecology*, 1:325–363, 1971.

[15] S. Jamshidi, H. Siebert, and A. Bockmayr. Preservation of dynamic properties in qualitative modeling frameworks for gene regulatory networks. *Biosystems*, 112(2):171–179, 2013.

[16] Z. Khalis, J.-P. Comet, A. Richard, and G. Bernot. The SMBioNet method for discovering models of gene regulatory networks. *Genes, Genomes and Genomics*, 3(1):15–22, 2009.

[17] J.-C. Leloup and A. Goldbeter. Toward a detailed computational model for the mammalian circadian clock. *PNAS*, 100(12):7051–7056, 2003.

[18] C. Schmal, J. Myung, H. Herzel, and G. Bordyugov. A theoretical study on seasonality. *Frontiers in Neurology*, 6(94), 2015.

[19] Y. Shigeyoshi, K. Taguchi, S. Yamamoto, S. Takekida, L. Yan, H. Tei, T. Moriya, S. Shibata, J. J. Loros, J. C. Dunlap, and H. Okamura. Light-induced resetting of a mammalian circadian clock is associated with rapid induction of the mPer1 transcript. *Cell*, 91(7):1043 – 1053, 1997.

[20] E. H. Snoussi and R. Thomas. Logical identification of all steady states: the concept of feedback loop characteristic states. *Bulletin of Mathematical Biology*, 55(5):973–991, 1993.

[21] R. Thomas. Boolean formalization of genetic control circuits. *Journal of Theoretical Biology*, 42(3):563–585, 1973.

[22] R. Thomas. Regulatory networks seen as asynchronous automata: a logical description. *Journal of Theoretical Biology*, 153(1):1–23, 1991.

[23] S. Troncale, J.-P. Comet, and G. Bernot. Verification of biological models with timed hybrid Petri nets. In *Proc. of the 2007 Intl. Symp. on Computational Models for Life Sciences (CMLS07), ISBN 978-0-7354-0466-3*, volume 952, pages 287–296, Australia, 2007, December 17-19.

[24] K. Vanselow and A. Kramer. Role of phosphorylation in the mammalian circadian clock. In *Cold Spring Harbor symposia on quantitative biology*, volume 72, pages 167–176. Cold Spring Harbor Laboratory Press, 2007.

[25] U. Wilensky. Netlogo. `http://ccl.northwestern.edu/netlogo/`, Center for Connected Learning and Computer-Based Modeling, Northwestern University. Evanston, IL, 1999.

[26] S.-H. Yoo, S. Yamazaki, P. L. Lowrey, K. Shimomura, C. H. Ko, E. D. Buhr, S. M. Siepka, H.-K. Hong, W. J. Oh, O. J. Yoo, et al. Period2::luciferase real-time reporting of circadian dynamics reveals persistent circadian oscillations in mouse peripheral tissues. *PNAS USA*, 101(15):5339–5346, 2004.